MS accepted/published at Marine Geology, doi: 10.1016/j.margeo.2017.05.003

Formation of sediment waves by turbidity currents and geostrophic flows: A discussion

I.N. McCave
Godwin Laboratory for Palaeoclimate Research, Department of Earth Sciences,
Downing Street, Cambridge CB2 3EQ, UK.

Abstract

A condition for the existence of sediment waves under turbidity currents as antidunes with the requirement of a slope gradient $\geq 3.0 \times 10^{-3}$ is deduced. Data show no such waves on slopes $< 2.5 \times 10^{-3}$, but some contourite mudwaves occur on slopes as low as 4.4×10^{-4}. However the latter also occur on slopes $> 3 \times 10^{-3}$ so no clear distinction is possible. Where turbidity current channels cross sediment drifts, or geostrophic flows traverse turbidite fans, the origin of most mudwaves will need to be determined by reference to internal features and context. A key problem is deposition of mud as antidunes from turbidity currents where even the waning flow is probably well above the critical *erosion* velocity for a *clear* flow. Deposition must occur from high concentration flows well above clear water critical depositional stresses. Once a wavy bed is set up, subsequent deposition may occur via the lee-wave mechanism proposed for contourite waves under a gradient Froude Number >1. A steep angle (<45°) between crest and flow axes is typical of GF waves, which may be dunes or antidunes, whereas TC waves tend to be orthogonal, but data on this discriminant are sparse.

Keywords

mudwaves, sediment waves, antidunes, contourites, turbidity currents, geostrophic flow.

Highlights

- Turbidity current sediment waves should (do) not exist on slopes less than $3x10^{-3}$.
- Contourite mudwaves can exist on lower gradients but there is no clear distinction.
- Turbidite antidune muds are deposited at stresses above critical for clear water.
- Angles between mudwave crest and geostrophic flow directions are typically <45°.

1. Introduction

Deep-sea sediment waves, also known as mud waves, are symmetrical bedforms with internal stratification indicating a sense of migration counter to the prevailing depositional flow in the majority of cases. They thus resemble the shallow water bedforms known as antidunes, and indeed, one of the first recognitions of them referred to 'abyssal antidunes' (Fox et al., 1968). They occur under turbidity current (TC) and geostrophic flow (GF) systems. The names are used interchangeably here, though for GF (contourite) waves 'mudwave' is preferred because they are almost always entirely of mud (90% < 63 μm plus sand-sized foraminifera). Large areas of deep-sea fans and contourite drifts are mantled with these bedforms. Contourite mud waves have wavelengths mainly in the range L = 1 to 2.5 km, but in the Argentine Basin examples are about 5 km. Turbidite mud waves can be of lower wavelength (but sandy), while most occurrences on levees and open slopes are mud-dominated and lie between L = 0.75 and 2.5 km (Symons et al., 2016). Such wavelengths are compatible with the expression of Hand et al. (1972):

$$L = 2\pi U^2(\rho_t + \rho_f)/g\Delta\rho$$

where U is flow speed, and $\Delta\rho$ is the density difference between the current ρ_t and overlying fluid ρ_f. Allen (1984) also deduces a criterion for turbidity current flow thickness h:

$$L/4\pi < h < L/2\pi$$

which gives thicknesses of 60-400 m for the larger modal range. Trough-to-crest heights for both types average around 20-30 m but can range up to 200 m and down to <5 m, with a broad wavelength to height scale dependence.

What can sediment wave bedforms tell us about the depositing flow conditions under turbidity currents and geostrophic flows? It is very difficult to distinguish between sediment waves found under turbidity currents (TC) and deep geostrophic flows (GF) other than by context. Turbidite fans and contourite drifts are tolerably distinguishable, but turbidity currents can traverse drifts and geostrophic flows pass over fans. Most waves have been observed in 3.5 kHz or old echo sounder profiles where information on orientation is lacking. With modern swath bathymetry in deep water a swath width ≈ 5 times water depth wide is generally achieved, able to resolve sediment waves, so bedform orientation with respect to the slope can now be assessed.

The principal mechanism proposed for formation of TC waves is antidunes under a supercritical flow (Normark et al., 1980), and for formation of GF waves the lee-wave mechanism of Flood (1988) with later modifications is now accepted. The TC mechanism almost always occurs with downslope flow (and upslope-migrating waves) whereas the GF mechanism can operate with flow having either an up- or down-slope component of a dominantly along-slope current, and wave migration both with (dune) and counter (antidune) to the sense of flow known to occur (Hopfauf & Spiess, 2001). Certainly most waves of whatever type appear to migrate with an upslope component [see papers in Wynn & Stow (2002a)]. There have been several reviews of deep sea sediment wave morphology and settings (Wynn & Stow, 2002b; Symons et al., 2016) so this aspect is not treated here. Rather, some aspects of flow dynamics leading to wave formation, mud deposition, and criteria for distinguishing mudwaves are explored.

2. Antidunes and Turbidity currents

The condition for formation of antidunes under a flow with a free surface is given by Kennedy (1963) as:

$$\mathrm{Fr} = U/(gh)^{1/2} \geq 1 \qquad (1)$$

and for a subsurface gravity current the density contrast enters the expression in 'reduced gravity' g' = (g $\Delta\rho/\rho_t$)

$$\mathrm{Fr} = U/(g'h)^{1/2} \geq 1 \qquad (2)$$

where Fr is the Froude number, $\Delta\rho = (\rho_t - \rho_w)$, U is flow speed averaged over the whole flow, h is flow depth (or thickness for a subsurface flow), g is acceleration due to gravity, and ρ_t and ρ_w are the mean densities of the turbid flow and ambient clear water respectively.

Flow speed of turbidity current body down a slope S is:

$$U = \left[\frac{g'hS}{C_D(1+a)}\right]^{1/2} \qquad (3)$$

where C_D is the quadratic drag coefficient $((\tau/\rho_t)/U^2)$ in which τ is the boundary shear stress and α is the ratio of the drag at the top to the base of the flow, often given as ~0.5 (Ippen & Harleman, 1962; Komar, 1969).

From (2), in the limiting case of Fr = 1: $\quad g'h = \left(\frac{U}{Fr}\right)^2$

So in (3), $\quad U = \left[\frac{U^2}{Fr^2}\,\frac{S}{C_D(1+a)}\right]^{1/2} = \frac{U}{Fr}\left(\frac{S}{C_D(1+a)}\right)^{1/2}$

Therefore, $Fr = \left(\frac{S}{C_D(1+a)} \right)^{1/2}$ (4)

If the drag coefficient takes the value $C_D = 2 \times 10^{-3}$ (for deep flow over a transitional to rough bed (Bird et al., 1982)), with $\alpha = 0.5$ and $Fr \geq 1$, then $S \geq 3 \times 10^{-3}$ (0.17°: degrees are used in the Symons et al. (2016) data base) to form antidunes.

So, whatever the flow density or height h, the slope must be > ~3×10^{-3} to form antidunes, and going down a decreasing slope, those mudwaves which are antidunes caused by supercritical flow should die out before or at a gradient of ~3×10^{-3} .

It is observed that as the gradient declines you lose antidunes downslope. In the Selvage wave field north of the Canary Islands (Wynn et al., 2000), waves die out as slope declines below 2.8×10^{-3}, which is very close to prediction. Similarly, on the Demerara slope sediment waves disappear as the slope declines to less than 2.96×10^{-3} (0.17°) (Gonthier et al., 2002). One might turn this around and observe that the choice of drag coefficient is not too far wrong.

3. Difficulty of mud deposition

There is a problem though; to get the mudwaves you have to deposit mud. For deposition from ***dilute*** suspensions, rather slow flow speeds are needed, generally < 0.20 m s^{-1}. Almost all estimates of turbidity current flow properties yield speeds well in excess of this value, a problem that was realised by Normark et al. (1980). They went to great lengths to find parameters that would yield slow speeds in order to fulfil the critical deposition stress requirement but with $Fr \geq 1$, and suggested very low concentrations indeed, namely those found in concentrated deep sea nepheloid layers; 10^{-6} to 10^{-5} by volume, ~2-20 g m^{-3}. In the light of many models of turbidity current flow (e.g. Dade & Huppert, 1995) this is too low. Initial volume concentrations of ~5×10^{-2} and runout values down to 10^{-3} (≈ 2 kg m^{-3}) are more likely.

For gravity flows under commonly deduced dimensions and concentrations (e.g. Dade & Huppert, 1995), at the lower limit for antidunes, high velocity is implied, e.g. with the standard equation (3) above; assuming $h = 100$ m, $\rho_t = 1130$ kg m^{-3}, $\rho_w = 1050$ kg m^{-3},

($\Delta\rho$ = 80 kg m^{-3} ($\equiv$ ~5% by volume, C ~ 130 kg m^{-3})), g = 9.8 m s^{-2} , with $C_D(1+\alpha) = 3.10^{-3}$, yields U = 8.3 m s^{-1} on a slope of 3.10^{-3}, Fr = 1.0. Even in the waning phase of a large flow with the above parameters but h = 10 m, U is 2.6 m s^{-1}. The relatively low velocity TCs deduced for a channel on Gardar Drift by Parnell-Turner et al. (2015), using both eq (3) and the cross channel Coriolis slope equation of Komar (1969), have U ~ 2 m s^{-1} and C ~10 kg m^{-3} (ρ_t = 1045 kg m^{-3}, ρ_w = 1039 kg m^{-3}, $\Delta\rho$ = 6 kg m^{-3}). Now these speeds are well above the critical erosion velocity for all sediment below gravel size under clear water (Miller et al., 1977), even for aged mud (Winterwerp and van Kesteren, 2004), so the density at the downstream end of the waning flow must have been less, probably C <10 kg m^{-3}, and/or deposition occurred well above clear water critical erosion stress values.

Two other factors should be considered that allow mud to be deposited from flows faster than predicted for low concentration. First, 10 kg m^{-3} is in the 'hindered settling' condition where high concentration of mud is argued to suppress turbulence in turbidity current flow (McCave & Jones, 1988). However, these conditions lead eventually to a plug flow (zero vertical velocity gradient) of unsorted sediment with a sheared base of coarser material. Alternatively, experiments at moderate concentration (1 kg m^{-3}) show that mud deposition can occur at boundary shear stresses at least four times those that allow deposition from low concentration flows (Mehta & Partheniades, 1973). Now C = 1 kg m^{-3} is not a very high concentration (0.04 % by volume) so in the absence of relevant experimental evidence (but with model insight from Zeng & Lowe, 1997), it is probable that mud is deposited from 10-100 kg m^{-3} (0.4-4%) flows at stresses >10x clear water values, i.e. > 2 Pa given by speeds of >1.0 m s^{-1}.

An additional solution to this problem might be to set up the antidunes with a concentrated flow depositing sand at Fr > 1, followed by a late stage of less concentrated suspension flow that lays down a drape over the bed at low speed, as advocated by Wynn and Stow (2002b). These waves continue with the antidune form -- internal acoustic reflections in most cases show up-current migration of the bedforms. The well known turbidite mudwaves on Bounty Fan (Carter et al., 1990) were shown by drilling to have sandy bases with mud tops where the upper 16 mbsf has 38% sand and 16-119 mbsf has just 26% sand and 74% mud (Shipboard Scientific Party, 1990). The waves migrate towards the channel (i.e. against the direction of overspill) on both banks and are thus antidunes (Fig. 1). In these cases the bulk of the turbidites are fine grained and it is unlikely that deposition occurred slowly (months) from dilute tail ends of the flows. More likely is that deposition was from the

decelerating body of a flow with high concentration of mud. This would accommodate the requirements of flow fast enough for both Fr ≥ 1 for antidunes and mud deposition.

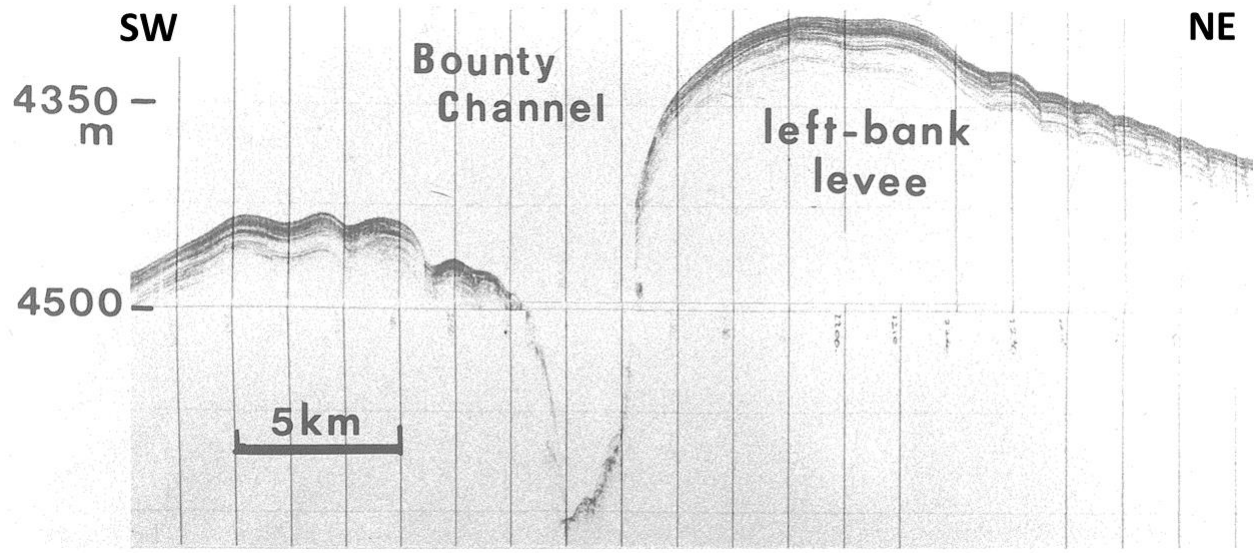

Fig. 1. Mudwaves on the levees of Bounty Fan (from Carter et al., 1990). Channel flow is toward the reader and the SW Pacific boundary current flows from SW to NE across the fan. Nevertheless, waves on both banks migrate towards the channel and are thus related to turbidity current overspill from the channel (see also Carter et al. (1990) Fig. 7).

The Froude Numbers above are bulk flow values, calculated for a uniform top-to-bottom concentration. Possibly a stratified suspension with a gradient Froude No. (Miles and Huppert, 1968), $Fr_{grad} = U/Nh$, with N the buoyancy frequency $(-(g/\rho_w)d\rho_t/dz)^{½}$; $Fr_{grad} = U/h(-(g/\rho_w)\, d\rho_t/dz)^{½}$ >1 would allow a type of supercritical flow at low sediment concentrations. Because $d\rho/dz$ is very small assuming a linear change in density over the flow thickness (a change in density of 10 kg m^{-3} over a 100 m thick flow with $\rho_w \sim 1050$ yields a denominator of 0.032), Fr_{grad} is >>1. A 100 kg m^{-3} change over 100 m gradient yields a denominator of 0.1, so Fr_{grad} is always >1 and even a slow relatively dilute suspension flowing over mudwaves will be in the supercritical regime and reinforce the growth of *already existing mudwaves* (the mechanism does not initiate the waves).

4. **Gradients**

The local gradients under which mudwaves are recorded were compiled by Normark et al. (2002) for turbidites, and recently a comprehensive database of all waves has been assembled by Symons et al. (2016) with additions here. Data are plotted as histograms of slope in logarithmic sequence in Fig. 2. A sharp cut-off in TC slopes and the presence of GF mudwaves on slopes as low as 0.025° (4.4 x 10^{-4}) is evident. This provides strong support for the initial premise that mudwaves need a slope > 0.003 to form antidunes under turbidity currents.

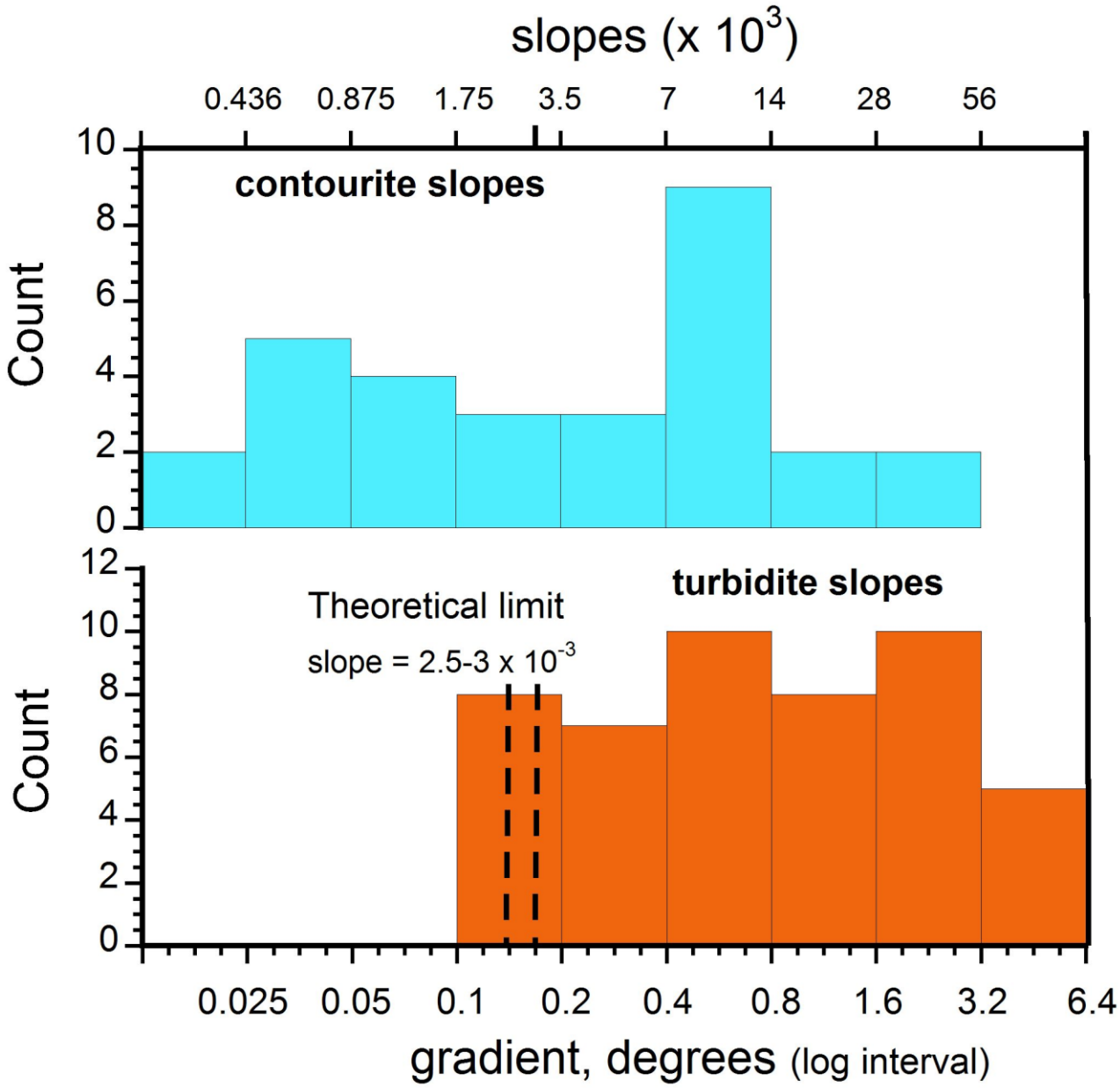

Fig. 2. Sea-bed gradients at sites of mudwave occurrence on open slopes and distal fans from the databases of Normark et al. (2002), and Symons et al. (2016) (Table 1). Gradients are on a logarithmic scale. Gradients of steep fan channels with high speed

flows have not been included. Note the sharp cut-off in TC slopes and the presence of GF mudwaves on slopes as low as 4.4 x 10^{-4} (0.025°).

It also allows some mudwaves at least to be assigned to a geostrophic flow origin when they occur on slopes < ~ 0.002, but there is no clear distinction on the basis of slope.

5. The conditions for abyssal mudwaves under geostrophic currents

In Flood's (1988) lee-wave mechanism he showed that κ ($=1/Fr_{grad}$) ranged from 0.4 to 1.5 for a thermohaline stratified flow over sediment waves on the Blake Outer Ridge, where κ is the inverse of the gradient Froude number, expressed as $\kappa = (Nh/U_g)$, where N is the stability, h is the wave trough-to crest height (height of a semi-circular bump in the analysis of Miles & Huppert (1968)) and U_g is the free-stream (geostrophic) velocity). As Fr_{grad} for present-day flow over these waves is about 1, in many cases such sediment waves can be regarded as antidunes and indeed they mostly have an up-current component of migration, though they are rarely normal to flow direction (as assumed by Flood). Blumsack & Weatherly (1989) extended the theory to deal with non-orthogonal wave to flow direction to give the condition for mudwave growth as $|f/k| < U < |N/k|$, where f is the Coriolis parameter, and the wave number $k = 2\pi/L$ (L is the mud-wavelength). For the Argentine Basin conditions this corresponded to wavelengths between 1 and 6 km. A further elaboration of the theory by Hopfauf and Spiess (2002) gives the orientations and wavelengths for maximum mudwave growth.

5.1 Orientation

Could orientation discriminate between mudwave types? Theoretical analyses of waves under geostrophic flow indicate that they may be oblique (left or right) to the dominant flow direction (Blumsack & Weatherley, 1989; Hopfauf & Spiess, 2001), and observations show they generally are, generally at an angle[1] < 45° (see references in Supp. Info), whereas TC mudwave crests tend to be parallel to the slope. In the southern hemisphere mudwave crests lie mainly to the left of the flow (but only 8 records) while they are both to the right

[1] The angle here is that between the flow direction and the crest trend of the mudwave. To avoid the ambiguity caused by not all mudwaves being antidunes (which have a component of their motion counter to the flow), Table 1 indicates whether the example is an antidune or a dune (with a component of migration downcurrent). The flow direction is along slope; see Fig. S1 for explanation.

and left in the north (Table 1). Whereas the great majority are antidunes, some are dunes with a component of their motion in the direction of flow (e.g. Hatton Drift waves analysed by MacLachlan et al, (2008); and some on Feni Drift (Roberts and Kidd, 1979)). Although measurements of current are on the 1 year time scale and wave growth is on at least a 10^5 year scale, the flow direction, being controlled by overall topography, is likely unchanged on the 1 Ma time scale. In a few cases the long-term flow direction is given by superimposed furrows (Hollister et al, 1974; Embley et al, 1980). Bianchi & McCave (2000) note that for mudwaves on Gardar Drift "The orientation of their axes inferred from swath bathymetry …. is at ~20° anticlockwise relative to the local bathymetry regardless of their position in relation to the crest of Gardar Drift." These observations generally agree with those of Manley and Caress (1994), (Table 1).

The migration sense of waves is usually fairly clear – it can be with or against (more common) the current or zero, i.e. upward growth – and usually upslope. Many current-formed waves lie at an acute angle to the current, a feature that might be thought useful for determining origin. However, on a continental margin where waves migrate upslope and make an acute angle (<20°) with flow direction (e.g. off Argentina (Gruetzner et al., 2014)) they may be confused with those formed by turbidity currents or draped downslope creep (Cattaneo et al., 2004). Orientation of the crest at an angle <45° relative to the flow direction is still a useful but not infallible discriminant between TC and GC flow mechanisms.

6. Conclusions

Whatever the density or thickness of a turbidity current, the slope must be greater than about 3×10^{-3} to form antidunes, and going down a decreasing slope, those mudwaves which are antidunes caused by supercritical flow should die out before or at a gradient of $\sim 3 \times 10^{-3}$.

A problem is that to get mudwaves you have to deposit mud, and slow flow speeds, generally < 0.20 m s^{-1}, were thought to be required based on low-concentration critical deposition conditions. Possible ways out of this difficulty are (i) high concentration of mud suppresses turbulence in turbidity current flow and (ii) at high concentration mud deposition occurs at boundary shear stresses many times those that allow deposition from low concentration. A further possibility is that fast flows set up the antidunes depositing sand, followed by a later stage of lower concentration turbidity current flow that lays down a drape over the bed at lower speed.

For contourite mudwaves, a gradient Froude Number for present-day thermohaline flow over some waves is about $Fr_{grad} = 1$, thus in many cases such sediment waves can be regarded as antidunes, and they have an upcurrent component of migration. GF mudwave crests are most commonly oriented at an oblique angle (of <45° to left or right) to the direction of flow, and may be dunes or antidunes, but this is not an infallible discriminator.

Acknowledgements

I am most grateful to Prof. Peter Talling and Dr William Symons for access to their sediment waves database for modern systems. Dr. Lionel Carter kindly supplied the profile of the Bountu Channel levees. I also appreciate the positive resonse of the referees to the thoughts expressed here.

References

Allen, J.R.L., 1984. *Sedimentary structures, their character and physical basis*. Vol I, Elsevier, Amsterdam, 593 p.

Bianchi G.G., McCave, I.N., 2000. Hydrography and sedimentation under the deep western boundary current on Björn and Gardar Drifts, Iceland Basin. *Mar. Geol.* **165**, 137–169.

Bird, A.A., Weatherly G.L., Wimbush M., 1982. A study of the bottom boundary-layer over the Eastward scarp of the Bermuda Rise. *J. Geophys Res.* **87**, 7941-7954.

Blumsack, S.L., Weatherly, G.L., 1989. Observations of the nearby flow and a model for the growth of mudwaves. *Deep-Sea Res*. **36**, 1327-1339.

Carter, L., Carter, R.M., Nelson, C.S., Fulthorpe, C.S., Neil, H.L., 1990. Evolution of Pliocene to Recent abyssal sediment waves on Bounty Channel levees, New Zealand. *Mar. Geol.* **95**, 97–109.

Cattaneo, A., Correggiari, A., Marsset, T., Thomas, Y., Marsset, B., Trincardi, F., 2004. Seafloor undulation pattern on the Adriatic shelf and comparison to deep-water sediment waves. *Mar. Geol*. **213**, 121-148.

Dade, W.B., Huppert, H.E., 1995. A box model for non-entraining, suspension-driven gravity surges on horizontal surfaces. *Sedimentology* **42**, 453-471.

Embley, R.W., Hoose, P.J., Lonsdale, P., Mayer, L., Tucholke, B.E., 1980. Furrowed mudwaves on the western Bermuda Rise. *Geol. Soc. America Bull.* **91**, 731 – 740.

Flood, R.D., 1988. A lee-wave model for deep-sea mudwave activity. *Deep-Sea Res.* **35**, 973-983.

Fox, P.J., Heezen, B.C. and Harian, A.M., 1968. Abyssal antidunes. Nature 220, 470-472.

Gonthier, E., Faugères, J.C., Gervais, A., Ercilla, G., Alonso, B., Baraza, J., 2002. Quaternary sedimentation and origin of the Orinoco sediment-wave field on the Demerara continental rise (NE margin of South America). *Mar. Geol*. **192**, 189–214.

Gruetzner, J., Uenzelmann-Neben, G., Franke, D., Arndt, J. E., 2014. Slowdown of Circumpolar Deepwater flow during the Late Neogene: Evidence from a mudwave field

at the Argentine continental slope. *Geophys. Res. Lett.* **41**, 2070–2076, doi:10.1002/2014GL059581.

Hand, B. M., Middleton, G. V. and Skipper, K., 1972. Antidune cross-stratification in a turbidite sequence, Cloridorme Formation, Gaspe, Quebec. *Sedimentology*, **18**,135-138.

Hollister, C.D., Flood, R.D., Johnson, D.A., Lonsdale, P.F., Southard, J.B., 1974. Abyssal furrows and hyperbolic echo traces on the Bahama Outer Ridge. *Geology* **2**, 395-400.

Hopfauf, V., Spiess V., 2001. A three-dimensional theory for the development and migration of deep sea sedimentary waves. *Deep-Sea Res. I* **48**, 2497-2519.

Ippen, A.T., Harleman D.R.F., 1952. Steady-state characteristics of subsurface flow, *National Bureau Standards (U.S.) Circular* **521**, 79-93.

Kennedy, J.F., 1963. The mechanics of dunes and antidunes in erodible-bed channels. *J. Fluid Mech.* **16**, 521-540.

Komar, P.D., 1969. Channelized flow of turbidity currents with application to Monterey deep-sea fan channel. *J. Geophys Res.* **74**, 4544-4560.

MacLachlan, S.E., Elliott, G.M., Parson, L.M., 2008. Investigations of the bottom current sculpted margin of Hatton Bank, NE Atlantic. *Mar. Geol.* **253**, 170–184.

Manley, P.L., Caress, D.W., 1994. Mudwaves on the Gardar sediment drift, NE Atlantic. *Paleoceanography* **9**, 973-988.

McCave, I.N., Jones, K.P.N., 1988. Deposition of ungraded muds from high-density, non-turbulent turbidity currents. *Nature* **333**, 250-252.

Mehta, A.J., Partheniades, E. 1973. *Depositional Behaviour of Cohesive Sediments*. Coastal and oceanographic engineering laboratory, University of Florida, Gainesville, Tech. Rept. No. 16, 274pp.

Miles, J. W., Huppert, H.E., 1968. Lee waves in a stratified flow. Part 2. Semi-circular obstacle. *J. Fluid Mech.* **33**, 803-814.

Miller, M.C., McCave, I.N. and Komar, P.D., 1977 Threshold of sediment motion under unidirectional currents. *Sedimentology* **24**, 507-527.

Normark, W.R., Hess, G.R., Stow, D.A.V., Bowen, A.J., 1980. Sediment waves on the Monterey Fan levees: a preliminary physical interpretation. *Mar. Geol*. **37**, 1-18.

Normark W.R., Piper D.J.W., Posamentier H., Pirmez C., Migeon S.L., 2002. Variability in form and growth of sediment waves on turbidite channel levees. *Mar. Geol.*, **192**, 23-58.

Parnell-Turner, R., White N.J., McCave, I.N., Henstock T.J., Murton, B., Jones, S.M., 2015. Architecture of North Atlantic contourite drifts modified by transient circulation of the Icelandic mantle plume. *Geochem., Geophys., Geosyst.* **16**, 3414–3435, doi: 10.1002/2015GC005947

Roberts, D.G., Kidd, R.B., 1979. Abyssal sediment wave fields on Feni Ridge, Rockall Trough: Long-range sonar studies. *Mar. Geol.* **33**, 175-191.

Shipboard Scientific Party, 1999. 6. Site 1122: Turbidites with a contourite foundation, In Carter, R.M., McCave, I.N., Richter, C., Carter, L., et al., *Proc. Ocean Drilling Program, Initial Reports* **181**, 146 p. doi:10.2973/odp.proc.ir.181.106.2000.

Symons, W.O., Sumner, E.J., Talling, P.J., Cartigny, M.J.B., Clare, M.A., 2016. Large-scale sediment waves and scours on the modern seafloor and their implications for the prevalence of supercritical flows. *Mar. Geol.* **371**, 130–148.

von Lom-Keil, H., Spiess, V., Hopfauf, V., 2002. Fine-grained sediment waves on the western flank of the Zapiola Drift, Argentine Basin: evidence for variations in Late Quaternary bottom flow activity. *Mar. Geol.* **192**, 239-258.

Winterwerp, J.C. & van Kesteren, W.G.M., 2004. *Introduction to the Physics of Cohesive Sediment in the Marine Environment*. Elsevier, Amsterdam, 466 p.

Wynn R.B., Stow D.A.V., (eds), 2002a. Recognition and interpretation of deep-water sediment waves: implications for palaeoceanography, hydrocarbon exploration and flow process interpretation. *Mar. Geol.* **192**, (1-3), 1-333.

Wynn, R.B., Stow, D.A.V., 2002b. Classification and characterisation of deep-water sediment waves. *Mar. Geol.* **192**, 7-22

Wynn, R.B., Weaver, P.P.E., Ercilla, G., Stow, D.A.V., Masson, D.G., 2000. Sedimentary processes in the Selvage sediment-wave field, NE Atlantic: new insights into the formation of sediment waves by turbidity currents. *Sedimentology* **47**, 1181–1197.

Zeng, J.J., Lowe, D.R., 1997. Numerical simulation of turbidity current flow and sedimentation: I. Theory. *Sedimentology* 44, 67-84.

Table 1. Gradients of Mudwave fields from Symons et al. (2016), Normark et al. (2002) and present additions.

Turbidite , unconfined			Contourite						
	degrees	slope (x 10^{-3})		degrees	slope (x 10^{-3})	Flow -to-crest angle	Hemi-sphere	Dune, Up or Antidune	ref
Cilaos	0.10	1.75	SW Bermuda	0.001	0.0175	28° L	N	AD	4
Humboldt	0.12	2.09	Zapiola Drift #6	0.001	0.0175	20° L	S	AD	6
Selvege	0.13	2.27	Ewing Drift	0.029	0.506	20°-40° L	S	AD, some D	5
Orinoco	0.14	2.44	Argyro Drift	0.030	0.524	?	S	AD	5
Hikurangi	0.15	2.62	Zapiola Drift	0.034	0.593	?	S	AD	5
Demerara	0.17	2.97	Surinam shelf	0.036	0.625	26° L	N	D	1
Cilaos	0.20	3.49	Falkland Tr	<0.049	0.871	~ 45° L	S	AD	3
Hikurangi	0.20	3.49	Gardar 'A' (N)	0.058	1.005	8° R	N	D	12
Selvege	0.22	3.84	Falkland Tr	0.060	1.047	~ 45° L	S	AD	3
Dongsha	0.28	4.89	Gardar 'B'	0.060	1.047	33° L	N	D	12
Hikurangi	0.30	5.24	Zapiola Drift #5	0.089	1.563	45° L	S	AD	6
Hikurangi	0.30	5.24	Gardar 'D'	0.120	2.094	12° R	N	AD	12
Hikurangi	0.30	5.24	Gardar 'A' (S)	0.171	2.990	83° R	N	AD	12
Dongsha	0.31	5.41	S. Gardar	0.171	3.000	51° L	N	U	2
Landes	0.40	6.98	N. Gardar	0.25	4.35	53° L	N	D	2
La Palma	0.40	7.00	Gardar 'C'	0.250	4.363	10° R	N	AD	12
Toyama	0.41	7.16	Bahama O.R.	0.300	5.236	31° R	N	AD	7
Dongsha	0.46	8.03	Feni Drift	0.425	7.43	17° L	N	AD	13
Orinoco	0.48	8.38	Feni Drift	0.426	7.44	10° L	N	U	13
Dongsha	0.51	8.90	Amirante Pass.	0.445	7.77	?	S	U	9
La Palma	0.55	9.60	S. Gardar	0.463	8.081	28° L	N	U	2
Amazon Fan	0.57	10.00	Morocco	0.500	8.727	30° R	N	AD	10
Hikurangi	0.60	10.47	Feni Drift	0.504	8.8	48° L	N	AD	13
Amazon Fan	0.69	12.00	Feni Drift	0.506	8.83	38° R	N	AD	13
Lake superior	0.74	13.00	Feni Drift	0.563	9.83	12°-36° L	N	D	13
Monterey	0.80	14.00	Weddell	0.782	13.66	12°-40° L	S	AD	8
Lake superior	1.15	20.00	Weddell	1.175	20.50	12°-40° L	S	AD	8
Var	1.15	20.00	Hatton Drift	1.500	26.18	33° L	N	D	11
Amazon Fan	1.15	20.07	Hatton Drift	2.000	34.91	35° L	N	D	11
Noeick	1.20	20.94	Hatton Drift	2.000	34.91	20° L	N	D	11
Toyama	1.38	24.00							
Cilaos	1.50	26.18							
Rockall Tr	1.50	26.18							
La Palma	1.72	30.00							
Dongsha	2.00	34.91							
Gabon	2.00	34.91							
Var	2.01	35.00							
Barra fan	2.29	40.00							
S. Sandwich	2.50	43.63							
Dongsha	3.00	52.36							
Gabon	3.00	52.36							
Rockall Tr	3.00	52.36							
Landes	3.00	52.36							
Noeick	3.60	62.83							
Var	3.72	65.00							
Dongsha	4.00	69.81							
Gabon	4.00	69.81							
S China Sea slope	5.46	95.29							

L= crest to left of flow
R= crest to right of flow
U = Upward growth
? = unknown (crest or flow or both)
1,2,…. 13; References in Supp. Info.

Supplementary Information

Contourite mudwave references, for Table 1 in main text.

1. Allersma, E., 1971, Mud on the oceanic shelf off Guyana. In: *Symposium on Investigations and Resources of Caribbean Sea and Adjacent Regions*, UNESCO, Paris, 193-203.
2. Bianchi G.G., McCave, I.N., 2000. Hydrography and sedimentation under the deep western boundary current on Björn and Gardar Drifts, Iceland Basin. *Mar. Geol.* **165**, 137–169.
3. Cunningham A.P., Barker P.F., 1996. Evidence for westward-flowing Weddell Sea Deep Water in the Falkland Trough, western South Atlantic. *Deep-Sea Research I* **43**, 643-654
4. Embley, R.W., Hoose, P.J., Lonsdale, P., Mayer, L., Tucholke, B.E., 1980. Furrowed mud waves on the western Bermuda Rise. *Geol. Soc. America Bull.* **91**, 731 - 740 ,
5. Flood, R.D., Shor, A.N., 1988. Mud waves in the Argentine Basin and their relationship to regional bottom circulation patterns. *Deep-Sea Res*. **35**, 943-972.
6. Flood, R.D., Shor, A.N., Manley, P.L., 1993. Morphology of abyssal mud waves at Project MUDWAVES sites in the Argentine Basin. Deep-Sea Res. II **40**, 859-888.
7. Hollister, C.D., Flood, R.D., Johnson, D.A., Lonsdale, P.F., Southard, J.B., 1974. Abyssal furrows and hyperbolic echo traces on the Bahama Outer Ridge. *Geology* **2**, 395-400
8. Howe, J.A., Livermore, R.A., Maldonado, A., 1998. Mudwave activity and current-controlled sedimentation in Powell Basin, northern Weddell Sea, Antarctica. *Mar. Geol*. **149**, 229–241
9. Johnson, D.A. & Damuth, J.E., 1979. Deep thermohaline flow and current-controlled sedimentation in the Amirante Passage: western Indian Ocean. *Mar. Geol.*, **33**: 1-44.
10. Lonsdale, P., 1983. Sediment drifts of the Northeast Atlantic and their relationship to the observed abyssal currents. *Bulletin de l'Institut de Geologie du Bassin d'Aquitaine* **31**, 141-149.
11. MacLachlan, S.E., Elliott, G.M., Parson, L.M., 2008. Investigations of the bottom current sculpted margin of Hatton Bank, NE Atlantic. *Mar. Geol.* **253**, 170–184.
12. Manley, P.L., Caress, D.W., 1994. Mudwaves on the Gardar sediment drift, NE Atlantic. *Paleoceanography* **9**, 973-988.
13. Roberts, D.G., Kidd, R.B., 1979. Abyssal sediment wave fields on Feni Ridge, Rockall Trough: Long-range sonar studies. *Mar. Geol.* **33**, 175-191.
14. Weatherly, G.L., 1993. On deep-current and hydrographic observations from a mudwave region and elsewhere in the Argentine Basin. *Deep-Sea Res. Part II* 40, 939-961.

Supplementary Fig. 1. Crest and flow orientations of contourite mudwaves.

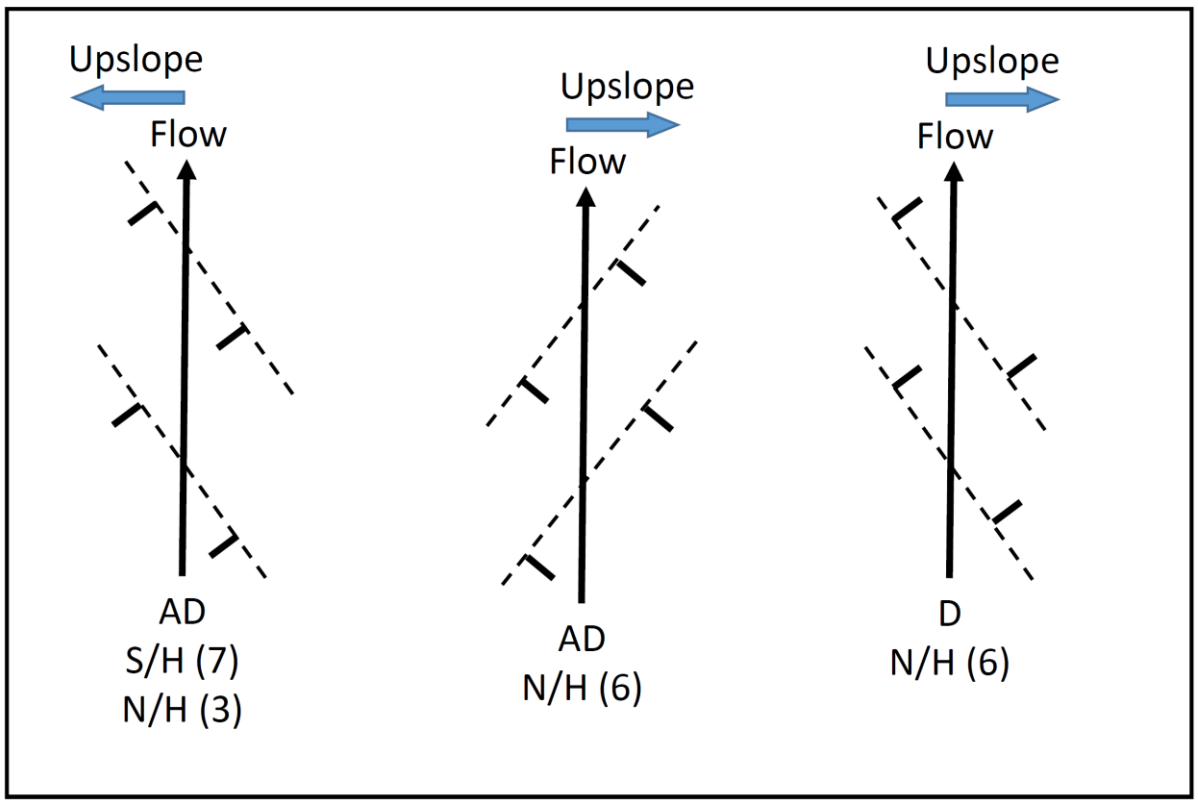

Dashed lines indicate the crest orientations and ticks mark the migration direction of the waves. AD = antidune, D = dune. Numbers of occurrences (in brackets) of the different orientations and senses of movement for Southern Hemisphere (S/H) and Northern Hemisphere (N/H) are drawn from Table 1. (Total examples are S/H – 8; N/H – 20 (of which 4 are Up))